ISSN 0021-3640, JETP Letters, 2016, Vol. 104, No. 8, pp. 578–587. © Pleiades Publishing, Inc., 2016.
Original Russian Text © A.V. Burmistrova, I.A. Devyatov, 2016, published in Pis'ma v Zhurnal Eksperimental'noi i Teoreticheskoi Fiziki, 2016, Vol. 104, No. 8, pp. 593–603.

SCIENTIFIC SUMMARIES

Theory of Coherent Charge Transport in Junctions Involving Unconventional Superconducting Materials

A. V. Burmistrova[a–d] and I. A. Devyatov[b, c, *]

[a] *Faculty of Physics, Moscow State University, Moscow, 119991 Russia*
[b] *Skobeltsyn Institute of Nuclear Physics, Moscow State University, Moscow, 119991 Russia*
[c] *Moscow Institute of Physics and Technology (State University), Dolgoprudnyi, Moscow region, 141700 Russia*
[d] *Moscow State Pedagogical University, Moscow, 119992 Russia*
**e-mail: igor-devyatov@yandex.ru*

Received September 13, 2016

Recent theoretical studies of coherent charge transport in junctions involving unconventional superconducting materials such as high-temperature superconducting iron-based pnictides (FeBS) and in structures with induced superconductivity which are formed of a thin metal layer with spin–orbit coupling in contact with an *s*-wave superconductor (S_{SO}) are reported. The theoretical analysis is performed with our unified approach based on the tight-binding method and boundary conditions obtained for it. This approach makes it possible to take into account a complex nonparabolic and anisotropic spectrum of normal excitations in unconventional superconducting materials and their multiband character, as well as unusual types of symmetries of the superconducting order parameter in them. The possibility of a semiclassical description in the case of intraorbital superconducting pairing is demonstrated. The method of calculations and their results are presented for the conductivities of junctions between a normal metal and unconventional superconducting materials, as well as for the Josephson current. Comparison with the experiment for the junction with FeBS is performed and indicates the presence of the unusual $s_{\pm}$ symmetry of the order parameter. An experiment is proposed to test our theoretical results for S_{SO}.

DOI: 10.1134/S0021364016200091

Investigation of new unconventional superconducting materials such as high-temperature iron-based superconducting pnictides (FeBS) [1], superconducting perovskites Sr_2RuO_4 [2], doped superconducting topological insulators $Cu_xBi_2Se_3$ [3], and also heterostructures consisting of a semiconductor with spin–orbit coupling or a topological insulator in contact with a conventional *s*-wave superconductor [4] is of great current interest. In FeBS, antiferromagnetism and superconductivity can paradoxically coexist, unconventional types of superconducting pairing caused by both spin fluctuations [5] (this type of pairing corresponds to the $s_{\pm}$ symmetry of the order parameter sign alternating over energy bands) and orbital fluctuations [6] with the s_{++} symmetry of the order parameter sign constant over energy bands were predicted, and the possibility of interorbital pairing was considered [7]. The chiral *p*-wave symmetry of the order parameter in Sr_2RuO_4 was predicted [2]. The possibility of appearance of the so-called Majorana modes [4], which can be used in a fault-tolerant quantum computer, at the edges of doped superconducting topological insulators $Cu_xBi_2Se_3$ [3] and S_{SO} was predicted. Efficient methods of studying unconventional superconducting materials, including the determination of the symmetry of the order parameter, are tunneling spectroscopy [8] and investigation of phase dependences of the Josephson current in various types of superconducting junctions with such materials [9, 10].

Common properties of the new unconventional superconducting materials listed above with both intrinsic and induced superconductivity are many bands in their energy spectra, a complex nonquadratic spectrum of single-electron excitations, and a superconducting order parameter expectedly anisotropic and sign-alternating over bands. For this reason, it is reasonable to describe coherent charge transport in their junctions with various materials within a universal method involving these features listed above. This approach developed recently in our works [11–16] is described in this review. Previous theories of coherent charge transport in such structures [4, 17–36] are phenomenological.

The review is organized as follows. First, we present the idea of our approach based on the tight-binding method with our boundary conditions for charge

transport in a single-orbital one-dimensional junction between a normal metal and a superconductor (N/S junction). Further, we demonstrate the application of this method to calculate charge transport in an N/S_p junction of FeBS with a normal metal, which is described within a two-orbital model of FeBS for various orientations of the iron planes of FeBS with respect to the interface. We demonstrate the possibility of the semiclassical description of such a transport problem in the case of intraorbital pairing in a multiband superconductor under the semiclassical condition, i.e., the smallness of the magnitude of the superconducting order parameter as compared to the Fermi energy and hopping parameters in the crystal lattice. Next, we describe a method for the calculation of the Josephson current in multiorbital superconductors by the tight-binding method and apply this method to calculate the phase and temperature dependences of the Josephson current in the S/S_p junction for various orientations of the crystallographic axes of FeBS with respect to the interface. Comparison with the experiment is performed. Coherent charge transport in the S_{SO} structure with induced superconductivity is theoretically studied and its Hamiltonian is microscopically obtained and is used to calculate the normal and Josephson currents for various types of junctions involving S_{SO}. Finally, the results of the work are summarized and conclusions are made.

We demonstrate our tight-binding method in application to the simplest model problem for the junction between the normal metal and superconductor (Fig. 1).

In the case of superconducting pairing of states at one site (orbital), the electron $u_{\nu,n}$ and hole $v_{\nu,n}$ amplitudes satisfy the discrete tight-binding equations [12]

$$\begin{cases} t_n u_{\nu,n+1} + t_{n-1} u_{\nu,n-1} + \Delta_n v_{\nu,n} - \mu u_{\nu,n} = \varepsilon_\nu u_{\nu,n}, \\ t_n v_{\nu,n+1} + t_{n-1} v_{\nu,n-1} - \Delta_n^* u_{\nu,n} - \mu u_{\nu,n} = -\varepsilon_\nu v_{\nu,n}. \end{cases} \quad (1)$$

These equations generalize the Bogoliubov–de Gennes equation to the case of a discrete lattice [37].

We showed in [11, 12] that the discrete description of transport in terms of tight-binding theory in the junction between a normal metal with identical hopping parameters between cells t' at zero superconducting pairing potential $\Delta_n = 0$, $n \le 0$ (left part of Fig. 1, filled red circles) and a superconductor described by a homogeneous order parameter $\Delta_n = \Delta$, $n \ge 1$, and identical hopping parameters between cells t (right part of Fig. 1, open blue circles) with the interface described by the hopping parameter γ is similar to the known Blonder–Tinkham–Klapwijk theory [38], which was previously formulated only in the continuum limit. To this end, we used an approach known in the theory of semiconductors [39], which makes it possible to coherently match discrete wavefunctions on atoms described within the tight-binding method.

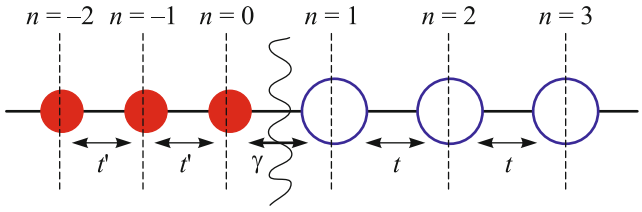

Fig. 1. (Color online) Scheme of the one-dimensional cell of atoms of the N/S structure.

The approach proposed in [39] is not limited by the assumption of a quadratic spectrum of normal excitations in contacting materials and is formally reduced to the matching of the equation for the left metal (Eq. (1) with $\Delta_n = 0$) continued to one cell behind the interface with the equation including hoppings through the interface and vice versa for the right metal (Fig. 1):

$$\begin{cases} t'\Phi_1 = \gamma\Psi_1, \\ \gamma\Phi_0 = t\Psi_0. \end{cases} \quad (2)$$

Here, the discrete electron wavefunctions $\Phi_n (= u_{\nu,n})$ for $n \le 0$ describe the left metal and the wavefunctions $\Psi_n (= u_{\nu,n})$ for $n \ge 1$ refer to the right metal. In the continuum limit, the discrete boundary conditions (2) are transformed to the known boundary conditions [40–42] obtained in the effective mass approximation. The boundary conditions given by Eqs. (2) ensure the conservation of the probability flux J through the interface [11, 12]:

$$\begin{aligned} J_{n<-1} &= \frac{2t'}{\hbar}\mathrm{Im}(\Phi_{n+1}^*\Phi_n) \\ &= J_{n>0} = \frac{2t}{\hbar}\mathrm{Im}(\Psi_{n+1}^*\Psi_n). \end{aligned} \quad (3)$$

Similarly, using the method proposed in [39] and the boundary conditions (2), one can obtain from Eqs. (1) the following boundary conditions for the junction between the normal metal and superconductor (Fig. 1):

$$\begin{cases} t'\Phi_1 = \gamma\Psi_1, \\ t'\bar{\Phi}_1 = \gamma\bar{\Psi}_1, \\ \gamma\Phi_0 = t\Psi_0, \\ \gamma\bar{\Phi}_0 = t\bar{\Psi}_0. \end{cases} \quad (4)$$

Here, the discrete wavefunctions $\Psi_n(\Phi_n)$ describe the electron states in the right (left) metal, as in Eqs. (2), whereas the wavefunctions $\bar{\Psi}_n(\bar{\Phi}_n)$ describe the respective hole states:

$$\begin{cases} \Phi_n = \exp(iq_1 nl) + b\exp(-iq_1 nl), \\ \bar{\Phi}_n = a\exp(iq_2 nl), \\ \Psi_n = cu\exp(iknl) + d\tilde{u}\exp(i\tilde{k}nl), \\ \bar{\Psi}_n = cv\exp(iknl) + d\tilde{v}\exp(i\tilde{k}nl). \end{cases} \quad (5)$$

The wavefunctions in the normal metal and superconductor contain four unknowns a, b, c, and d. The unknowns a and b describe waves Andreev and normally reflected to the normal metal, respectively, whereas the unknowns c and d describe waves passed to the superconductor. These four unknowns (a, b, c, and d) are unambiguously determined from the boundary conditions (4). In Eqs. (5), l is the distance between atoms of the normal metal and superconductor (for simplicity, we assume that all these distances are the same, but this assumption is not necessary [39]), and q_1, q_2, k, $\tilde{k}$ are the wave vectors in the normal metal and superconductor, which correspond to the energy E of propagating waves. These wave vectors are determined from the solutions of the spatially homogeneous Bogoliubov–de Gennes equations (1) for the normal metal and superconductor. The electron and hole Bogoliubov coefficients u, v; $\tilde{u}$, $\tilde{v}$ corresponding to waves propagating in the superconductor with the wave vector k; $\tilde{k}$ are also determined from solutions of the spatially homogeneous equations (1) with $\Delta_n = \Delta$.

It can be shown [11, 12] that the wavefunctions obtained with the use of the boundary conditions (5) ensure the conservation of the probability flux through the $J = J_s$ interface. The expression for the probability flux J_s in the one-dimensional lattice (Fig. 1) follows from the discrete Bogoliubov–de Gennes equations (1):

$$J_s = \frac{2}{\hbar}\mathrm{Im}(t\Psi^*_{n+1}\Psi_n - t\bar{\Psi}^*_{n+1}\bar{\Psi}_n). \quad (6)$$

The above consideration in the tight-binding approximation concerns an equilibrium situation with zero voltage drop V at the N/S interface. The proposed model can be generalized to the case of a finite voltage $V \neq 0$ across a microcontriction with sizes much smaller than the elastic l_{el} and inelastic l_{in} mean free paths, when charge transport occurs through independent transverse modes. The current flowing in each mode is determined by the difference between the incoming $f^{\rightarrow}(E)$ and outgoing $f^{\leftarrow}(E)$ electron fluxes in the normal metal [38]:

$$I(V) = \eta_1 \int \{f^{\rightarrow}(E) - f^{\leftarrow}(E)\}dE, \quad (7)$$

where $f^{\rightarrow}(E) = f_0(E - eV)$, $f_0(E)$ is the equilibrium Fermi distribution, $\eta_1 = e/(\pi\hbar)$, and

$$f^{\leftarrow}(E) = A(E)(1 - f^{\rightarrow}(-E)) + B(E)f^{\rightarrow}(E) + (C(E) + D(E))f_0(E). \quad (8)$$

Here, $A(E)$ is the probability of Andreev reflection of a hole from the normal metal to an electron, $B(E)$ is the probability of normal reflection of the electron, and $C(E)$ and $D(E)$ are the probabilities of the transmission of electron- and hole-like quasiparticles from the superconductor to the electron states of the normal metal, respectively. The probabilities A, B, C, and D appearing in Eq. (8) are determined from the boundary conditions (4) and Eqs. (3) and (6) for the probability flux. When calculating the probabilities A, B, C, and D, the incident quasiparticle states should be normalized so that the probability flux in these states given by Eqs. (3) and (6) would be unity. Such a normalization ensures thermodynamic equilibrium at zero voltage $V = 0$ at the N/S junction.

Charge transport through the junction between the normal metal and an unconventional single-orbital superconductor, e.g., a two-dimensional d-wave superconductor, can be described similarly. Such a description in our work [12] demonstrated that the results of the known work [43] are reproduced by our tight-binding method.

We now consider charge transport through the interface between the normal metal and multiband superconductor. As a multiband superconductor, we take FeBS (N/S_p interface) described within a two-orbital $s_{\pm}$ model [44]. The Hamiltonian matrix in the basis $\mathbf{B}_{\mathrm{orb}} = \{d^+_{k,x,\uparrow}, d^+_{k,y,\uparrow}, d_{-k,x,\downarrow}, d_{-k,y,\downarrow}\}$, where the operator $d^+_{k,x,\uparrow}$ ($d^+_{k,y,\uparrow}$) creates an electron with the quasimomentum $\mathbf{k}$ and the spin projection σ on the $3d$ $xz(yz)$ orbital, for an unfilled Brillouin zone has the form [45]

$$\mathbf{H}(\mathbf{k}) = \begin{pmatrix} \xi_{xx}(\mathbf{k}) & \xi_{xy}(\mathbf{k}) & \Delta_{\pm}(\mathbf{k}) & 0 \\ \xi_{xy}(\mathbf{k}) & \xi_{yy}(\mathbf{k}) & 0 & \Delta_{\pm}(\mathbf{k}) \\ \Delta_{\pm}(\mathbf{k}) & 0 & -\xi_{xx}(\mathbf{k}) & -\xi_{xy}(\mathbf{k}) \\ 0 & \Delta_{\pm}(\mathbf{k}) & -\xi_{xy}(\mathbf{k}) & -\xi_{yy}(\mathbf{k}) \end{pmatrix}. \quad (9)$$

Here, the matrix elements $\xi_{xx}(\mathbf{k}) = -2t_2\cos k_x - 2t_1\cos k_y - 4t_3\cos k_x\cos k_y - \mu$, $\xi_{yy}(\mathbf{k}) = -2t_1\cos k_x - 2t_2\cos k_y - 4t_3\cos k_x\cos k_y - \mu$ describe single-electron excitations on orbitals; the matrix element $\xi_{xy}(\mathbf{k}) = 4t_4\sin k_x\sin k_y$ describes the hybridization of orbitals, where t_i are the hopping amplitudes in FeBS and k_y, k_x are the components of the quasimomentum; and the matrix element $\Delta_{\pm}(\mathbf{k}) = \Delta_0\cos k_x\cos k_y$ describes intraorbital superconducting pairing corresponding to the $s_{\pm}$ model.

We first consider charge transport in the ab plane of FeBS in the absence of disorientation of crystallographic axes of FeBS with respect to the interface ((100)-oriented junction, Fig. 2).

The Bogoliubov–de Gennes equations at sites of the crystal lattice follow from Hamiltonian (9) and have the form

$$\begin{cases} t_1(\Psi^{\alpha}_{n+1,m}+\Psi^{\alpha}_{n-1,m})+t_2(\Psi^{\alpha}_{n,m+1}+\Psi^{\alpha}_{n,m-1})+\mu\Psi^{\alpha}_{n,m}+t_3(\Psi^{\alpha}_{n+1,m+1}+\Psi^{\alpha}_{n-1,m-1}+\Psi^{\alpha}_{n+1,m-1} \\ +\Psi^{\alpha}_{n-1,m+1})+t_4(-\Psi^{\beta}_{n+1,m+1}-\Psi^{\beta}_{n-1,m-1}+\Psi^{\beta}_{n+1,m-1}+\Psi^{\beta}_{n-1,m+1})+\Delta_0(\bar{\Psi}^{\alpha}_{n+1,m+1} \\ +\bar{\Psi}^{\alpha}_{n-1,m-1}+\bar{\Psi}^{\alpha}_{n+1,m-1}+\bar{\Psi}^{\alpha}_{n-1,m+1})=-E\Psi^{\alpha}_{n,m}, \\ t_2(\Psi^{\beta}_{n+1,m}+\Psi^{\beta}_{n-1,m})+t_1(\Psi^{\beta}_{n,m+1}+\Psi^{\beta}_{n,m-1})+\mu\Psi^{\beta}_{n,m}+t_3(\Psi^{\beta}_{n+1,m+1}+\Psi^{\beta}_{n-1,m-1}+\Psi^{\beta}_{n+1,m-1} \\ +\Psi^{\beta}_{n-1,m+1})+t_4(-\Psi^{\alpha}_{n+1,m+1}-\Psi^{\alpha}_{n-1,m-1}+\Psi^{\alpha}_{n+1,m-1}+\Psi^{\alpha}_{n-1,m+1})+\Delta_0(\bar{\Psi}^{\beta}_{n+1,m+1}+ \\ +\bar{\Psi}^{\beta}_{n-1,m-1}+\bar{\Psi}^{\beta}_{n+1,m-1}+\bar{\Psi}^{\beta}_{n-1,m+1})=-E\Psi^{\beta}_{n,m}, \\ t_1(\bar{\Psi}^{\alpha}_{n+1,m}+\bar{\Psi}^{\alpha}_{n-1,m})+t_2(\bar{\Psi}^{\alpha}_{n,m+1}+\bar{\Psi}^{\alpha}_{n,m-1})+\mu\bar{\Psi}^{\alpha}_{n,m}+t_3(\bar{\Psi}^{\alpha}_{n+1,m+1}+\bar{\Psi}^{\alpha}_{n-1,m-1}+\bar{\Psi}^{\alpha}_{n+1,m-1} \\ +\bar{\Psi}^{\alpha}_{n-1,m+1})+t_4(-\bar{\Psi}^{\beta}_{n+1,m+1}-\bar{\Psi}^{\beta}_{n-1,m-1}+\bar{\Psi}^{\beta}_{n+1,m-1}+\bar{\Psi}^{\beta}_{n-1,m+1})-\Delta_0(\Psi^{\alpha}_{n+1,m+1} \\ +\Psi^{\alpha}_{n-1,m-1}+\Psi^{\alpha}_{n+1,m-1}+\Psi^{\alpha}_{n-1,m+1})=E\bar{\Psi}^{\alpha}_{n,m}, \\ t_2(\bar{\Psi}^{\beta}_{n+1,m}+\bar{\Psi}^{\beta}_{n-1,m})+t_1(\bar{\Psi}^{\beta}_{n,m+1}+\bar{\Psi}^{\beta}_{n,m-1})+\mu\bar{\Psi}^{\beta}_{n,m}+t_3(\bar{\Psi}^{\beta}_{n+1,m+1}+\bar{\Psi}^{\beta}_{n-1,m-1}+\bar{\Psi}^{\beta}_{n+1,m-1} \\ +\bar{\Psi}^{\beta}_{n-1,m+1})+t_4(-\bar{\Psi}^{\alpha}_{n+1,m+1}-\bar{\Psi}^{\alpha}_{n-1,m-1}+\bar{\Psi}^{\alpha}_{n+1,m-1}+\bar{\Psi}^{\alpha}_{n-1,m+1})-\Delta_0(\Psi^{\beta}_{n+1,m+1} \\ +\Psi^{\beta}_{n-1,m-1}+\Psi^{\beta}_{n+1,m-1}+\Psi^{\beta}_{n-1,m+1})=E\bar{\Psi}^{\beta}_{n,m}. \end{cases} \quad (10)$$

Here, the wavefunctions $\Psi^{\alpha(\beta)}_{n,m}$ and $\bar{\Psi}^{\alpha(\beta)}_{n,m}$ describe the electron and hole states, respectively. The superscript $\alpha(\beta)$ of the wavefunctions $\Psi^{\alpha(\beta)}_{n,m}$ of superconducting FeBS corresponds to the $d_{xz}(d_{yz})$ orbital. The subscripts n and m of the wavefunction $\Psi^{\alpha(\beta)}_{n,m}$ of FeBS describe the coordinates n_x and n_y of the sites of the crystal lattice, respectively (see Fig. 2).

Similar to the derivation of the boundary conditions (4) but with allowance for independent hoppings to the d_{xz} and d_{yz} orbitals of FeBS (Fig. 2), we obtained in [11, 12] the following boundary conditions for the (100) N/S_p junction:

$$\begin{cases} t'\Phi_1=\gamma_1\Psi^{\alpha}_1+\gamma_2\Psi^{\beta}_1, \\ t'\bar{\Phi}_1=\gamma_1\bar{\Psi}^{\alpha}_1+\gamma_2\bar{\Psi}^{\beta}_1, \\ \gamma_1\Phi_0=(t_1+2t_3\cos k_y)\Psi^{\alpha}_0+2it_4\sin k_y\Psi^{\beta}_0+2\Delta_0\cos k_y\bar{\Psi}^{\alpha}_0, \\ \gamma_1\bar{\Phi}_0=(t_1+2t_3\cos k_y)\bar{\Psi}^{\alpha}_0+2it_4\sin k_y\bar{\Psi}^{\beta}_0-2\Delta_0\cos k_y\Psi^{\alpha}_0, \\ \gamma_2\Phi_0=(t_1+2t_3\cos k_y)\Psi^{\beta}_0+2it_4\sin k_y\Psi^{\alpha}_0+2\Delta_0\cos k_y\bar{\Psi}^{\beta}_0, \\ \gamma_2\bar{\Phi}_0=(t_1+2t_3\cos k_y)\bar{\Psi}^{\beta}_0+2it_4\sin k_y\bar{\Psi}^{\alpha}_0-2\Delta_0\cos k_y\Psi^{\beta}_0, \end{cases} \quad (11)$$

where $\gamma_1(\gamma_2)$ are the hopping amplitudes through the interface to the $d_{xz}(d_{yz})$ orbital and t' is the hopping amplitude between atoms of the normal metal (Fig. 2). For clarity, we assume that the periods of the crystal lattices of the normal metal and FeBS are the same and equal 1. In view of the translational symmetry of the considered structure in the direction parallel to the interface, the component of the quasimomentum k_y parallel to the interface is conserved. In view of this translational symmetry, the second subscript corresponding to the coordinate of an atom in the direction parallel to the interface is omitted in the electron (hole) wavefunctions $\Psi^{\alpha(\beta)}_{n,m}$ ($\bar{\Psi}^{\alpha(\beta)}_{n,m}$).

The wavefunctions of the considered N/S_p junction are determined by six coefficients: two coefficients a and b describe waves Andreev and normally reflected

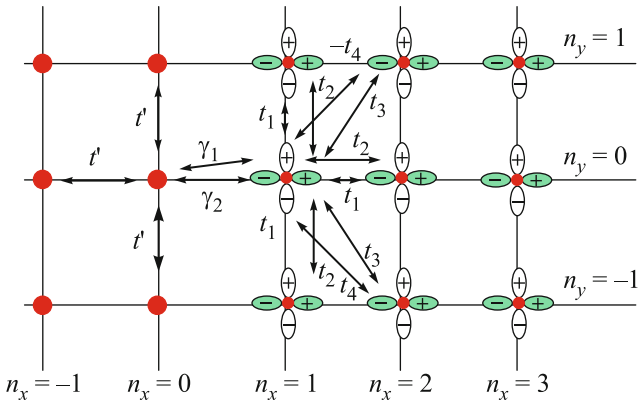

Fig. 2. (Color online) Two-dimensional atomic lattice representing the N/S_p interface in the (100) direction with zero disorientation angle between the interface and the crystallographic axes of FeBS.

to the normal metal, respectively, and four coefficients c_1, c_2, d_1, and d_2 correspond to waves passed to FeBS:

$$\begin{cases} \Phi_n = \exp(iq_1nl) + b\exp(-iq_1nl), \\ \bar{\Phi}_n = a\exp(iq_2nl), \\ \Psi_n^\alpha = c_1u_1(k_1)\exp(ik_1nl) + c_2u_1(k_2)\exp(ik_2nl) + d_1u_1(k_3)\exp(ik_3nl) + d_2u_1(k_4)\exp(ik_4nl), \\ \Psi_n^\beta = c_1u_2(k_1)\exp(ik_1nl) + c_2u_2(k_2)\exp(ik_2nl) + d_1u_2(k_3)\exp(ik_3nl) + d_2u_2(k_4)\exp(ik_4nl), \\ \bar{\Psi}_n^\alpha = c_1v_1(k_1)\exp(ik_1nl) + c_2v_1(k_2)\exp(ik_2nl) + d_1v_1(k_3)\exp(ik_3nl) + d_2v_1(k_4)\exp(ik_4nl), \\ \bar{\Psi}_n^\beta = c_1v_2(k_1)\exp(ik_1nl) + c_2v_2(k_2)\exp(ik_2nl) + d_1v_2(k_3)\exp(ik_3nl) + d_2v_2(k_4)\exp(ik_4nl), \end{cases} \quad (12)$$

where the wavefunctions $\Phi_n(\bar{\Phi}_n)$ describe the electron (hole) states in the normal metal. The wavefunctions given by Eqs. (12) correspond to the excitation of electron–hole states in FeBS by a single-electron state from the normal metal. The six coefficients a, b, c_1, c_2, d_1, and d_2 are unambiguously determined from six boundary conditions (11). The wave vectors q_1, q_2, k_i, $i = 1$–4 in the normal metal and superconductor correspond to the energy E of the propagating wave and are determined from the spatially homogeneous solutions of the Bogoliubov–de Gennes equations for the normal metal and FeBS (10), respectively. The electron and hole Bogoliubov coefficients $u_j(k_i), v_j(k_i)$ are also found from Eqs. (10). The number of waves passed to the normal metal is twice as large as that in the standard Blonder–Tinkham–Klapwijk model [38] because there are two bands in the considered model of FeBS [44].

The main problem in the numerical calculations is the determination of wave vectors $k_i(E)$ and Bogoliubov coefficients $u_j(k_i(E)), v_j(k_i(E))$ corresponding to a fixed energy E for waves propagating in FeBS from lengthy Eqs. (10). As was shown in [13], for the case of intraorbital pairing (including the popular $s_\pm$ and s_{++} models), a significant simplification corresponding to the so-called semiclassical approximation is possible when

$$\Delta_{\max} \ll t_i, \mu, \quad (13)$$

where $\Delta_{\max}$ is the maximum anisotropic order parameter. Condition (13) is usually satisfied in FeBS. Under condition (13), the Bogoliubov coefficients $u_j(k_i(E)), v_j(k_i(E))$ are factorized into the product of the usual Bogoliubov coefficients $u_0(E,\Delta)$, $v_0(E,\Delta)$ corresponding to conventional superconductors [37, 38] and coherent factors $\alpha(k_x,k_y)$, $\beta(k_x,k_y)$, which correspond to single-particle excitations in FeBS (the upper left 2×2 submatrix in the Hamiltonian matrix (9)) and are the solutions of the simple equation

$$\left(\begin{pmatrix} \xi_{xx}(\mathbf{k}) & \xi_{xy}(\mathbf{k}) \\ \xi_{xy}(\mathbf{k}) & \xi_{yy}(\mathbf{k}) \end{pmatrix} - E\right)\begin{pmatrix} \alpha(k_x,k_y) \\ \beta(k_x,k_y) \end{pmatrix} = 0, \quad (14)$$

at $E = 0$. The wave vectors in the semiclassical approximation are also determined from Eq. (14).

In the case of interorbital pairing [7], the semiclassical approximation in the above form is inapplicable.

The expression for the probability flux in the state with the fixed wave vector k_y in the direction parallel to the x axis follows from the Bogoliubov–de Gennes equations (10) at sites of the crystal lattice of FeBS:

$$\begin{aligned} J_p = \frac{2}{\hbar}\big((t_1 + 2t_3\cos k_y)\,\mathrm{Im}\{(\Psi_{n+1}^\alpha)^*\Psi_n^\alpha - (\bar{\Psi}_{n+1}^\alpha)^*\bar{\Psi}_n^\alpha\} \\ + (t_2 + 2t_3\cos k_y)\,\mathrm{Im}\{(\Psi_{n+1}^\beta)^*\Psi_n^\beta - (\bar{\Psi}_{n+1}^\beta)^*\bar{\Psi}_n^\beta\} \\ + 4t_4\sin k_y\,\mathrm{Re}\{(\Psi_{n+1}^\alpha)^*\Psi_n^\beta + (\Psi_{n+1}^\beta)^*\Psi_n^\alpha \\ - (\bar{\Psi}_{n+1}^\alpha)^*\bar{\Psi}_n^\beta - (\bar{\Psi}_{n+1}^\beta)^*\bar{\Psi}_n^\alpha\} + 2\Delta_0\cos k_y\,\mathrm{Im}\{(\Psi_{n+1}^\alpha)^*\bar{\Psi}_n^\alpha \\ + (\bar{\Psi}_{n+1}^\alpha)^*\Psi_n^\alpha + (\Psi_{n+1}^\beta)^*\bar{\Psi}_n^\beta + (\bar{\Psi}_{n+1}^\beta)^*\Psi_n^\beta\}\big). \end{aligned} \quad (15)$$

It was shown in [11, 12] that the boundary conditions (11) ensure the conservation of the flux through the N/S$_p$ interface $J = J_p$.

The Bogoliubov–de Gennes equations, boundary conditions, and the expression for the flux in the case of the s_{++} symmetry of the order parameter in FeBS, which is modeled by the potential $\Delta = 2\Delta_0(\cos k_x + \cos k_y) + \Delta_1$ [7], are determined similarly [12].

It is noteworthy that the phenomenological boundary conditions [18] obtained for junctions with multiband superconductors by analogy with a quantum waveguide follow from our microscopic approach only with allowance for additional "oblique" hoppings at the interface [12], which are not shown in Fig. 2, and only at a certain relation between the hopping parameters at the interface and in FeBS.

The current through the two-dimensional microcontriction between FeBS and metal is determined by Eq. (7) integrated over the transverse component of the quasimomentum k_y: $I_p(V) = \eta_2\int dk_y I(V,k_y)$, where $\eta_2 = \Xi/2\pi$ and Ξ are the characteristic sizes of the microcontriction. In the considered case, the probabilities C and D appearing in Eq. (7) are determined as the sums of probabilities from two bands:

$C = C_1 + C_2$, $D = D_1 + D_2$. The probabilities A, B, C_i, and D_i are calculated from the boundary conditions (11) and Eqs. (3) and (15) for the probability flux. When calculating the probabilities A, B, C_i, and D_i, the incident quasiparticle states should be normalized so that the probability flux in these states given by Eqs. (3) and (15) would be unity. Such a normalization ensures thermodynamic equilibrium at zero voltage $V = 0$ at the N/S_p junction.

The case of nonzero misorientation of the crystallographic axes of FeBS with respect to the N/S_p interface qualitatively differs from the case of zero misorientation. It is necessary to investigate transport in the N/S_p junction at nonzero misorientation. Indeed, the study of electron transport in junctions between the normal metal and superconducting cuprates with nonzero misorientation angles of the principal crystallographic axes of a cuprate and a metal contacting it provides the conclusion on the existence of the d symmetry of the order parameter in cuprates [43]. The coupling of the normal metal to FeBS through the interface was described by a larger number of hopping parameters than that at zero misorientation angle. In addition to the hopping parameters γ_1, γ_2 to the $d_{xz}(d_{yz})$ orbital of FeBS nearest to the N/S_p interface, additional hopping parameters γ_1', γ_2' through the interface had to be used [11, 12]. These hopping parameters through the interface take into account the coupling between the orbitals of the last layer of atoms in FeBS and the atomic layer of the normal metal next nearest to the interface. These processes should be taken into account because diagonal bonds in the crystal lattice of FeBS are broken at the interface for a nonzero disorientation angle. Moreover, diagonal hoppings in the square lattice t_2' in the normal metal had to be taken into account in addition to hoppings between the nearest neighbors t_1' [11, 12]. The mentioned circumstances significantly complicate the boundary conditions, wavefunctions, and expression for the flux, which differ from Eqs. (11), (12), and (15) corresponding to the case of zero misorientation angle [11, 12]. Furthermore, in the case of a nonzero misorientation angle, charge transport through the N/S_p interface occurs not only through two energy bands but also through two valleys in these bands.

The numerical calculations of the differential conductivities of N/S_p junctions showed [11, 12] that only two-gap voltage dependences of the conductance components with a fixed transverse quasimomentum k_y in the case of the s_{++} symmetry of the order parameter are observed for any orientation of the interface and for any k_y values. At the same time, additional subgap features for components of conductivities can appear in the case of the $s_{\pm}$ symmetry of the order parameter, absence of misorientation of interfaces, low conductance of the junction, and finite k_y values. These additional subgap features are due to a change in the sign of the superconducting pairing potential within the $s_{\pm}$ model in the presence of coupling between orbitals of FeBs at finite k_y values.

However, voltage dependences of the angle-averaged differential conductance are usually observed in real experiments. The angle-averaged differential conductance of N/S_p junctions without the misorientation of the interface for the s_{++} and $s_{\pm}$ symmetries of the order parameter of FeBs at various chemical potentials of the adjacent normal metal was numerically calculated in [12]. As was shown in [12], the s_{++} and $s_{\pm}$ symmetries can be distinguished only in the case of a large Fermi surface in the normal metal. We detected additional subgap peaks in the averaged conductance of low-transparent N/S_p junctions only for the $s_{\pm}$ symmetry. We revealed the suppression of the conductance for high transparent N/S_p junctions owing to destructive interference [18] at low voltages for the $s_{\pm}$ symmetry as compared to similar values for the s_{++} symmetry. Thus, in order to distinguish the s_{++} and $s_{\pm}$ symmetries in FeBS in tunnel experiments, it is necessary to use N/S_p junctions without the misorientation of the interface with a large Fermi surface in the N layer.

Josephson transport in homogeneous junctions between multiband superconductors and a spin-singlet single-orbital s-wave superconductor was similarly considered in [14, 15] in terms of hoppings in the crystal lattice and through the interface. As a multiband superconductor, we took FeBS, which is described within the two-orbital model [44], with the possible s_{++} and $s_{\pm}$ symmetries of the order parameter. For transport in ab iron planes in the (100) direction, the structure of orbitals and hoppings through the interface is similar to that shown in Fig. 2, where circles in the left part of Fig. 2 correspond in this case to an s-wave superconductor rather than to a normal metal, as was accepted in the preceding section. We considered an additional intermediate layer of a single-orbital insulator (I), which is not shown in Fig. 2. The coupling of the s-wave superconductor with the insulator is described by the hopping parameter γ and the coupling of the insulator with the $d_{xz}(d_{yz})$ orbitals of FeBS is described by the hopping parameters $\gamma_1(\gamma_2)$ through the interface. For clarity, we assumed that the periods of the crystal lattices of the s-wave superconductor, insulator, and FeBS are the same and equal 1.

To calculate the Josephson current through the junction, it is necessary to construct the Green's function of the entire junction. To this end, we constructed the lattice Green's functions for the S, I, and S_p regions and matched them at the interfaces by the

method developed in [11, 12]. The lattice Matsubara two-orbital Green's function is defined as [14, 15]

$$\mathbf{G}_{\{n\},\{j\}}(\tau_1,\tau_2)=\begin{pmatrix}\hat{G}_{\{n\},\{j\}}(\tau_1,\tau_2) & \hat{F}_{\{n\},\{j\}}(\tau_1,\tau_2)\\ \hat{\bar{F}}_{\{n\},\{j\}}(\tau_1,\tau_2) & \hat{\bar{G}}_{\{n\},\{j\}}(\tau_1,\tau_2)\end{pmatrix}, \quad (16)$$

where τ_i is the imaginary "time" and $\hat{G}_{\{n\},\{j\}}(\tau_1,\tau_2)$, $\hat{F}_{\{n\},\{j\}}(\tau_1,\tau_2)$, $\hat{\bar{G}}_{\{n\},\{j\}}(\tau_1,\tau_2)$, and $\hat{\bar{F}}_{\{n\},\{j\}}(\tau_1,\tau_2)$ are 4×4 matrices in the orbital space. The components of these matrices have the form

$$\begin{cases}G^{(\alpha\beta)}_{\{n\},\{j\}}(\tau_1,\tau_2)=-\langle T_\tau c^{(\alpha)}_\uparrow(\{n\},\tau_1)c^{(\beta)\dagger}_\uparrow(\{j\},\tau_2)\rangle,\\ F^{(\alpha\beta)}_{\{n\},\{j\}}(\tau_1,\tau_2)=\langle T_\tau c^{(\alpha)\dagger}_\downarrow(\{n\},\tau_1)c^{(\beta)\dagger}_\uparrow(\{j\},\tau_2)\rangle,\\ \bar{G}^{(\alpha\beta)}_{\{n\},\{j\}}(\tau_1,\tau_2)=-\langle T_\tau c^{(\alpha)\dagger}_\downarrow(\{n\},\tau_1)c^{(\beta)}_\downarrow(\{j\},\tau_2)\rangle,\\ \bar{F}^{(\alpha\beta)}_{\{n\},\{j\}}(\tau_1,\tau_2)=\langle T_\tau c^{(\alpha)}_\uparrow(\{n\},\tau_1)c^{(\beta)}_\downarrow(\{j\},\tau_2)\rangle.\end{cases} \quad (17)$$

Here, the superscripts α and β can be 1 and 2, which correspond to the d_{xz} and d_{yz} orbitals, respectively; $c^{(1)\dagger}_\sigma(\{n\},\tau_i)\left(c^{(2)\dagger}_\sigma(\{n\},\tau_i)\right)$ is the creation operator of an electron with the spin σ belonging to the d_{xz} (d_{yz}) orbital at the $\{n\}=(n_x,n_y)$ site; and T_τ is the operator of ordering in imaginary time.

The Green's functions $\mathbf{G}^{\mathbf{S}}$ and $\mathbf{G}^{\mathbf{I}}$of the conventional superconductor $\mathbf{G}^{\mathbf{S}}$ and insulator $\mathbf{G}^{\mathbf{I}}$ are similar to those given by Eqs. (16) and (17) but without orbital superscripts.

Similar to the above consideration of quasiparticle transport in N/S_p junctions, we obtained discrete lattice versions of the Gorkov equations for two-orbital Green's functions (16) and (17). Similar to the derivation of Eqs. (11), we arrived at the boundary conditions similar to Eqs. (11) and derived the equation for the current [14, 15]. Matching the Green's functions of the usual superconductor, insulator, and FeBS at the S/I and I/S_p interfaces with the use of the resulting boundary conditions, we constructed the unified Green's function of the $S/I/S_p$ junction by the method proposed in [46] and calculated the Josephson current [14, 15]. We demonstrated that the proposed discrete Green's functions technique in the single-orbital limit reproduces the known results obtained previously for Josephson junctions consisting of usual superconductors [47–52] and d-wave superconductors [53].

We similarly analyzed three-dimensional Josephson transport in the z direction in $S/I/S_p$ junctions by introducing additional hopping parameters t_z between orbitals of neighboring FeBS planes and the hopping parameters γ_{1z}, γ_{2z} through the I/S_p interface [14, 15].

Current–phase relations and temperature dependences of the Josephson current were numerically calculated in [14, 15] for various transport directions with respect to the crystallographic axes of FeBS, various lengths of the insulator, and various hopping parameters through the interface. The Fermi energy of the usual superconductor was chosen in the calculations such that the Fermi surface was large enough to cover all bands of the adjacent FeBS layer. The analysis of the current–phase relations showed that the $S/I/S_p$ junction in the case of the s_{++} symmetry in FeBS is always a 0 junction with the minimum free energy of the Josephson junction at zero phase difference at it. At the same time, at tunneling in the (100)-oriented $S/I/S_p$ junction in the case of the $s_\pm$ symmetry in FeBS, we predicted the presence of 0, π, and ϕ junctions, when the minimum free energy is reached at the phase difference at the junction equal to 0, π, and $0<\phi<\pi$, respectively. In this case, the most unconventional current–phase relations with a large contribution from the second harmonics and ϕ junctions are possible only in direct Josephson junctions without an insulator layer I with a significant thickness. Interband interference effects in the case of the $s_\pm$ symmetry are physically responsible for unconventional current–phase relations and a large contribution from the second harmonic.

The situation is different in the case of z-oriented $S/I/S_p$ junctions. In such direct junctions in the case of the $s_\pm$ symmetry, a π junction occurs, but it transforms to a 0 junction after addition of several atoms of the insulator I. This transformation can be experimentally detected by, e.g., placing such $S/I/S_p$ junctions in a SQUID, as was proposed recently in [54]. A significant suppression of the critical current in such junctions with a sufficiently thick insulator layer I was recently revealed experimentally [55]. In the case of the s_{++} symmetry in z-oriented $S/I/S_p$ junctions, a 0 junction always occurs.

Our calculations of the temperature dependence of the critical current $I_c(T)$ of the $S/I/S_p$ junction [15] gave quite simple monotonic dependences close to the Ambegaokar–Baratoff dependence [49] for the usual S/I/S junction. We detected the largest difference of $I_c(T)$ from the Ambegaokar–Baratoff dependence in the (100)-oriented direct $S/I/S_p$ junction at hopping parameters through the interface γ_1,γ_2 corresponding to a ϕ junction in it.

The amplitudes of microwave-induced steps on the current–voltage characteristic of the Josephson junction were measured in [15] as functions of the microwave power at voltages multiple of $\hbar\omega_{mw}/2e$, where ω_{mw} is the microwave frequency. The Josephson junction was made of FeBS with the composition $Ba_{0.4}K_{0.6}(FeAs)_2$ adjacent to a needle of the usual superconductor $Pb_{0.7}In_{0.3}$. The injection of the supercurrent either on ab iron planes in $Ba_{0.4}K_{0.6}(FeAs)_2$ or in the z direction was performed by varying the sharp-

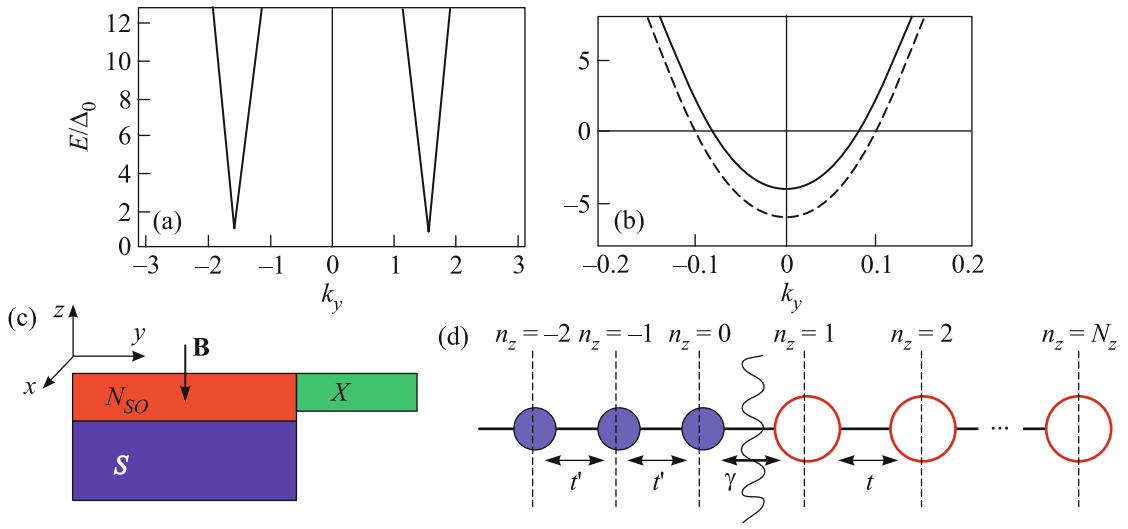

Fig. 3. (Color online) (a) Spectrum of quasiparticle excitations in the S layer. (b) Spectrum of quasiparticle excitations in the N_{SO} layer in the z direction. (c) Scheme of the considered heterostructure, where X can be N, S, or S_{SO}. (d) Scheme of the used tight binding model.

ness of the $Pb_{0.7}In_{0.3}$ needle. The measurements were performed at a temperature much lower than the critical temperature of $Pb_{0.7}In_{0.3}$. Using the standard method [56] and only one fitting parameter of coupling of microwave radiation with the junction [57], we demonstrated that the decisive contribution to current–phase relations in the case of injection of supercurrent in the z direction comes from the first harmonic $I \propto \sin(\varphi)$, whereas the decisive contribution to current–phase relations in the case of injection of supercurrent in the ab iron plane comes from the second harmonic $I \propto \sin(2\varphi)$. These experimental results confirm the $s_{\pm}$ symmetry of the superconducting order parameter in $Ba_{0.4}K_{0.6}(FeAs)_2$, because the above theory predicts such current–phase relations in the case of the injection of the supercurrent in the ab iron plane for most of the values of the hopping parameters γ_1, γ_2 through the interface in pure junctions. However, direct measurement of current–phase relations in such $S/I/S_p$ Josephson junctions is desirable.

In addition purely transport problems, we considered problems of induced superconductivity or proximity effect in heterostructures consisting of a metal with spin–orbit coupling (N_{SO}) or a topological insulator and a usual s-wave superconductor (see Fig. 3c). In [16], we showed that the effective one-dimensional Hamiltonian of the S/N_{SO} heterostructure written in the basis $\Psi = (\Psi^{SO,\uparrow}, \Psi^{SO,\downarrow}, \bar{\Psi}^{SO,\uparrow}, \bar{\Psi}^{SO,\downarrow})$ has the form

$$\widehat{H}_{\text{eff}} = \begin{pmatrix} \xi - h & \lambda k_y & \Delta_1(k_y) & \Delta_2(k_y) \\ \lambda k_y & \xi + h & -\Delta_2(k_y) & \Delta_3(k_y) \\ \Delta_1(k_y) & -\Delta_2(k_y) & -\xi + h & \lambda k_y \\ \Delta_2(k_y) & \Delta_3(k_y) & \lambda k_y & -\xi - h \end{pmatrix}, \quad (18)$$

which differs from the usual Hamiltonian [4, 35, 36, 58] because of the presence of triplet components of the order parameter $\Delta_1(k_y)$ and $\Delta_3(k_y)$ and the dependence on the wave vector of the induced superconducting order parameter $\Delta_i = \Delta_i(k_y)$. We showed that the triplet components of the order parameter $\Delta_1(k_y)$ and $\Delta_3(k_y)$ are odd functions of the wave vector k_y, whereas the singlet component $\Delta_2(k_y)$ is an even function of k_y. In Eq. (18), ξ is the energy of quasiparticle excitations, $h = g_e^* \mu_B B/2$ is the Zeeman energy corresponding to the magnetic field B applied in the z direction (see Fig. 3c), g_e^* is the Landé g-factor, μ_B is the Bohr magneton, and λ is the Rashba spin–orbit coupling constant [59]. Superconductivity in the N_{SO} layer is induced in the z direction owing to contact with the usual superconductor S, whereas transport occurs in the y direction to the material X, which can be the same heterostructure with induced superconductivity S_{SO}, a normal metal N, or a usual superconductor S (see Fig. 3c). To derive Eq. (18), we used the general approach described in [60] and adapted it for our tight-binding method [11, 12]. Using the boundary conditions (4) including the spin degrees of freedom, we matched the wavefunctions of the usual superconductor with eight bispinors, which describe the wavefunctions in N_{SO} [61] in the z direction at the S/N_{SO} interface and free boundary, and found the wavefunctions in N_{SO}. Further, using a standard procedure [37, 60], we constructed the retarded Green's function $\hat{G}(k_y)$ from the wavefunctions of the lower subband N_{SO} and found the Hamiltonian from the equation $-\hat{H}_{\text{eff}}(k_y)\hat{G}(k_y) = 1$. The resulting Hamilto-

nian is given by Eq. (18). The single-particle components of the Hamiltonian (18) (the upper left 2×2 submatrix in Eq. (18) and the lower right 2×2 submatrix in Eq. (18)) coincide with the respective initial component, which indicates that the derivation of Hamiltonian (18) is correct. The described procedure of derivation of the Hamiltonian of S_{SO} is the most general. It takes into account not only the spin–orbit coupling in the N_{SO} layer but also a finite transparency of the S/N_{SO} interface, thickness of the N_{SO} layer, and scattering from the interface between states of spin subbands. These important effects were disregarded in previous attempts [4, 35, 36] at deriving the effective Hamiltonian of S_{SO} involving the tunneling Hamiltonian in the momentum space.

Using the effective Hamiltonian (18), we confirmed well-known results for features in the conduction of the junction between this heterostructure and the normal metal (N/S_{SO} junction) at magnetic fields $h > h_c$ [62–64] and 4π periodicity of the Josephson current in a symmetric junction between two such heterostructures with induced superconductivity (S_{SO}/S_{SO} Josephson junction) [65], which are signatures of Majorana modes at the ends of such heterostructures [4]. At the same time, we demonstrated that Hamiltonian (18) gives very unconventional current–phase relations for a sufficiently transparent junction between heterostructures and a usual s-wave superconductor (S/S_{SO} Josephson junction). A decrease in the transparency of the S/S_{SO} interface results in usual sinusoidal current–phase relations. Such anomalous current–phase relations were predicted in our work [17] for the junction between a usual superconductor and a superconductor with interband pairing.

We demonstrated the possibility of the creation of considered heterostructures and Josephson junctions with the use of high-purity AlGaSb/InAs/AlGaSb heterostructures and niobium electrodes, as in [66, 67].

A similar analysis of the induced superconductivity and transport properties of a heterostructure consisting of a usual superconductor and a two-dimensional HgTe topological insulator [68] within the two-orbital model [69] with allowance for orbital degrees of freedom only confirmed known results [4] for quasiparticle and Josephson currents in junctions with such heterostructure, but did not give qualitatively new results.

To summarize, we have reported recent results [11–16] of theoretical description of coherent charge transport and the proximity effect in junctions with various unconventional superconducting materials within a unified approach based on the tight-binding method. The idea of the method has been described, results on quasiparticle and Josephson transport in junctions with FeBS have been reported, and induced superconductivity in N_{SO}, as well as quasiparticle and Josephson transport in heterostructures based on N_{SO}, has been analyzed. The method described in this work can be applied to interesting unsolved problems of charge transport in junctions with Sr_2RuO_4 within the three-band model, proximity effect, and charge transport in heterostructures consisting of three-dimensional topological insulators HgTe and Bi_2Se_3 in contact with a usual superconductor, proximity effect in heterostructures consisting of unconventional superconductors, e.g., FeBS in contact with N_{SO} and other interesting problems.

We are grateful to T.M. Klapwijk, M.Yu. Kupriyanov, Y. Tanaka, Y. Asano, A.S. Mel'nikov, and A.A. Golubov for stimulating discussion of the problem. This work was supported by the Russian Foundation for Basic Research (project no. 15-52-50054). The work of A.V.B. was supported by the Ministry of Education and Science of the Russian Federation (contract no. 14.B25.31.0007). The work of I.A.D. was supported by the Ministry of Education and Science of the Russian Federation (contract no. 14.Y26.31.0007).

REFERENCES

1. Y. Kamihara, T. Watanabe, M. Hirano, and H. Hosono, J. Am. Chem. Soc. **130**, 3296 (2008).
2. A. P. Mackenzie and Y. Maeno, Rev. Mod. Phys. **75**, 657 (2003).
3. Y. S. Hor, A. J. Williams, J. G. Checkelsky, R. Roushan, J. Seo, Q. Xu, H. W. Zandbergen, A. Yazdani, N. P. Ong, and R. J. Cava, Phys. Rev. Lett. **104**, 057001 (2010).
4. J. Alicea, Rep. Prog. Phys. **75**, 076501 (2012).
5. I. I. Mazin, D. J. Singh, M. D. Johannes, and M. H. Du, Phys. Rev. Lett. **101**, 057003 (2008).
6. H. Kontani and S. Onari, Phys. Rev. Lett. **104**, 157001 (2010).
7. A. Moreo, M. Daghofer, J. A. Riera, and E. Dagotto, Phys. Rev. B **79**, 134502 (2009).
8. E. L. Wolf, *Principles of Electron Tunneling Spectroscopy* (Oxford Univ. Press, Oxford, UK, 1985).
9. D. J. Van Harlingen, Rev. Mod. Phys. **67**, 515 (1995).
10. C. C. Tsue and J. R. Kirtley, Rev. Mod. Phys **72**, 969 (2000).
11. A. V. Burmistrova and I. A. Devyatov, JETP Lett. **96**, 391 (2012).
12. A. V. Burmistrova, I. A. Devyatov, A. A. Golubov, K. Yada, and Y. Tanaka, J. Phys. Soc. Jpn. **82**, 034716 (2013).
13. A. V. Burmistrova, I. A. Devyatov, A. A. Golubov, K. Yada, and Y. Tanaka, Supercond. Sci. Technol. **27**, 015010 (2014).
14. A. V. Burmistrova and I. A. Devyatov, Europhys. Lett. **107**, 67006 (2014).
15. A. V. Burmistrova, I. A. Devyatov, A. A. Golubov, K. Yada, Y. Tanaka, M. Tortello, R. S. Gonnelly, V. A. Stepanov, X. Ding, H.-H. Wen, and L. H. Green, Phys. Rev. B **91**, 214501 (2015).
16. A. V. Burmistrova, I. A. Devyatov, and I. E. Batov, Europhys. Lett. **114**, 57005 (2016).

17. A. V. Burmistrova and I. A. Devyatov, JETP Lett. **95**, 239 (2012).
18. M. A. N. Araújo and P. D. Sacramento, Phys. Rev. B **79**, 174529 (2009).
19. I. B. Sperstad, J. Linder, and A. Sudbø, Phys. Rev. B **80**, 144507 (2009).
20. J. Linder, I. B. Sperstad, and A. Sudbø, Phys. Rev. B **80**, 20503(R) (2009).
21. A. A. Golubov, A. Brinkman, Y. Tanaka, I. I. Mazin, and O. V. Dolgov, Phys. Rev. Lett. **103**, 077003 (2009).
22. I. A. Devyatov, M. Yu. Romashka, and A. V. Burmistrova, JETP Lett. **91**, 297 (2010).
23. A. V. Burmistrova, T. Yu. Karminskaya, and I. A. Devyatov, JETP Lett. **93**, 133 (2011).
24. A. V. Burmistrova, I. A. Devyatov, M. Yu. Kupriyanov, and T. Yu. Karminskaya, JETP Lett. **93**, 203 (2011).
25. W.-Q. Chen, F. Ma, Z.-Y. Lu, Z.-Y. Lu, and F.-C. Zhang, Phys. Rev. Lett. **103**, 207001 (2009).
26. E. Berg, N. H. Lindner, and T. Pereg-Barnea, Phys. Rev. Lett. **106**, 147003 (2011).
27. A. E. Koshelev, Phys. Rev. B **86**, 214502 (2012).
28. V. G. Stanev and A. E. Koshelev, Phys. Rev. B **86**, 174515 (2012).
29. Shi-Zeng Lin, Phys. Rev. B **86**, 014510 (2012).
30. Z. Huang and X. Hu, Appl. Phys. Lett. **104**, 162602 (2014).
31. S. Apostolov and A. Levchenko, Phys. Rev. B **86**, 224501 (2012).
32. C. Nappi, S. D. Nicola, M. Adamo, and E. Sarnelli, Europhys. Lett. **102**, 47007 (2013).
33. D. Wang, H.-Y. Lu, and Q.-H. Wang, Chin. Phys. Lett. **30**, 77404 (2013).
34. W.-F. Tsai, D.-X. Yao, B. A. Bernevig, and J. P. Hu, Phys. Rev. B **80**, 012511 (2009).
35. S. Tewari, T. D. Stanescu, J. D. Sau, and S. Das Sarma, New J. Phys. **13**, 065004 (2011).
36. A. C. Potter and P. A. Lee, Phys. Rev. B **83**, 184520 (2011).
37. A. B. Svidzinskii, *Spatially Inhomogeneous Problems in the Theory of Superconductivity* (Nauka, Moscow, 1982) [in Russian].
38. G. E. Blonder, M. Tinkham, and T. M. Klapwijk, Phys. Rev. B **25**, 4515 (1982).
39. Q.-G. Zhu and H. Kroemer, Phys. Rev. B **27**, 3519 (1983).
40. D.-J. BenDaniel and C. B. Duke, Phys. Rev. **152**, 683 (1966).
41. W.-A. Harrison, Phys. Rev. **123**, 85 (1961).
42. B. Laikhtman, Phys. Rev. B **46**, 4769 (1992).
43. Y. Tanaka and S. Kashiwaya, Phys. Rev. Lett. **74**, 3451 (1995).
44. S. Raghu, X.-L. Qi, C.-X. Liu, D. J. Scalapino, and S.-C. Zhang, Phys. Rev. B **77**, 220503(R) (2008).
45. M. M. Korshunov and I. Eremin, Phys. Rev. B **78**, 140509R (2008).
46. D. V. Goncharov, I. A. Devyatov, and M. Yu. Kupriyanov, J. Exp. Theor. Phys. **99**, 1074 (2004).
47. I. Kulik and A. N. Omel'yanchuk, Low Temp. Phys. **3**, 459 (1977).
48. I. Kulik and A. N. Omel'yanchuk, Low Temp. Phys. **4**, 142 (1978).
49. V. Ambegaokar and A. Baratoff, Phys. Rev. Lett. **10**, 486 (1963).
50. A. Furusaki and M. Tsukada, Solid State Commun. **78**, 299 (1991).
51. P. F. Bagwell, Phys. Rev. B **46**, 12573 (1992).
52. C. W. J. Beenakker and H. van Hauten, Phys. Rev. Lett. **66**, 3056 (1991).
53. Y. Tanaka and S. Kashiwaya, Phys. Rev. B **56**, 892 (1997).
54. A. A. Golubov and I. I. Mazin, Appl. Phys. Lett. **102**, 032601 (2013).
55. P. Siedel, Supercond. Sci. Technol. **24**, 043001 (2011).
56. A. Barone and G. Paternò, *Physics and Applications of the Josephson Effect* (Wiley, New York, 1982).
57. H. Sellier, C. Baraduk, F. Lefloch, and R. Calemczuk, Phys. Rev. Lett. **92**, 257005 (2004).
58. T. D. Stanescu and S. Tewari, J. Phys.: Condens. Matter **25**, 233201 (2013).
59. E. I. Rashba, Sov. Phys. Solid State **2**, 1109 (1960).
60. A. F. Volkov, P. H. C. Magnée, B. J. van Wees, and T. M. Klapwijk, Physica C **242**, 261 (1995).
61. T. Yokoyama, Y. Tanaka, and J. Inoue, Phys. Rev. B **74**, 035318 (2006).
62. T. D. Stanescu, J. D. Sau, R. M. Lutchyn, and S. Das Sarma, Phys. Rev. B **81**, 241310 (2010).
63. K. Flensberg, Phys. Rev. B **82**, 180516 (2010).
64. K. T. Law, P. A. Lee, and T. K. Ng, Phys. Rev. Lett. **103**, 237001 (2009).
65. R. M. Lutchyn, J. D. Sau, and S. Das Sarma, Phys. Rev. Lett. **105**, 077001 (2010).
66. J. Eroms and D. Weiss, Advances in Solid State Phys. **46**, 141 (2008).
67. F. Rohlfing, G. Tkachov, F. Otto, K. Richter, D. Weiss, G. Borghs, and C. Strunk, Phys. Rev. B **80**, 220507 (2009).
68. I. A. Devyatov and A. V. Burmistrova, in *Proceedings of the 5th International Conference on Fundamental Problems of High Temperature Superconductivity FPS-15, Oct. 5–9, 2015* (Fiz. Inst. AN, Moscow, 2015), p. 42.
69. B. A. Bernevig, T. L. Hughes, and S. C. Zhang, Science **314**, 1757 (2006).

Translated by R. Tyapaev